IV.04

Characterization of Stone Masonry Panels Consolidated by Injection of Grouts in Buildings Damaged by the 2009 Abruzzo Earthquake

Gilberto Artioli[1], Michele Secco[1], Claudio Mazzoli[1], Chiara Coletti[1], Maria Rosa Valluzzi[1] and Francesca da Porto[1]

[1] CIRCe – Centro Interdipartimentale di Ricerca per lo Studio dei Materiali Cementizi e dei Leganti Idraulici, University of Padova, Italy, gilberto.artioli@unipd.it, michele.secco@unipd.it, claudio.mazzoli@unipd.it, chiara.coletti@yahoo.it, valluzzi@dic.unipd.it, daporto@dic.unipd.it

Abstract This contribution is part of a research project aimed at developing a methodology for the emergency stabilization of historic buildings damaged by the 2009 Abruzzo earthquake through compatible injection grouts. Several portions of multi-leaf stone masonry walls from buildings in the towns of Onna, Tempera and Sant'Eusanio Forconese, all located near L'Aquila, were selected for experimental injection tests, planned and verified by means of multiscale characterization studies. The procedure and results of the preliminary studies on the historic mortars and the grouts are here reported. The materials were characterized from the petrographic, textural, mineralogical and chemical point of view through a multianalytical approach including petrographic examinations, particle size distribution studies, XRPD analyses, bulk chemical analyses by XRF and microchemical and microstructural studies by SEM-EDS. The original mortars were subdivided in different groups and a thorough knowledge of the chemical and mineralogical characteristics of the grouts was achieved, as background information for the restoration procedure according to the historic structures.

1 Introduction

The consolidation of damaged multi-leaf masonry walls constitutes one of the most challenging tasks for the structural stabilization of historic buildings, given the heterogeneous compositional nature and brittle mechanic behaviour of the structural elements. Grouting is the most common technique used for the restoration of damaged masonry walls, primarily for its property of maintaining

continuity between the constituents of the structures, while improving the deformability and mechanical properties without significant alteration to the morphology and load bearing system of the walls. Several studies regarding the use of injection grouts for the masonry restoration are reported in literature [1-4]. A few studies focus on the use of restoration products that differ from the classical cementitious and ternary grouts [5, 6], and generally they underestimate the importance of an adequate chemical-mineralogical characterization of the materials.

This contribution is part of a research project aimed at verifying the effectiveness of the emergency structural improvement of multi-leaf masonry walls damaged by the 2009 Abruzzo earthquake by means of compatible injection grouts to develop a protocol of intervention to apply in case of future earthquakes. Several portions of walls from six buildings in the towns of Onna (four buildings denominated CR, CB, VI, and BA), Tempera (TE), and Sant'Eusanio Forconese (SE), all located in the province of L'Aquila, were selected for experimental injection tests, planned and verified by means of non-destructive and destructive multiscale characterization studies. The original mortars of the six buildings were fully characterized from the petrographic, textural, mineralogical, and chemical points of view to select the most suitable restoration products. Then, six typologies of commercial injection grouts specifically designed for the restoration of historic masonry structures (denominated MI, M21, O2, O3, BC, and AI) were chosen and characterized through a multianalytical methodology similar to the one adopted for the characterization of the original materials. Moreover, the selected masonry portions were characterized by means of non-destructive sonic tests, and the shear strength and deformability of some of the masonry walls were evaluated by means of diagonal tests carried out in the non-reinforced state. The remaining masonry walls were injected with the selected grouts and then re-tested by means of sonic and diagonal compression tests in the strengthened state to assess the effectiveness of the interventions. The present contribution deals with the characterization of preliminary materials.

2 Characterization of the historic mortars

2.1 Materials and methods

A selection of mortars was sampled from the infilling leafs of the walls. A general homogeneity of mortar typology within each building was observed, hence a single mortar sample was analyzed for each structure. First, the samples were studied from a petrographic point of view, followed by analytical procedures for the study of mortar-based building materials described in UNI Norm 11176: 2006. A microscopical semi-quantitative determination of the material's total

porosity also was performed through comparison with visual estimation diagrams. Then, the binder and aggregate were separated [7], and the fraction with grain-size above 63 μm was dry-sieved according to standard UNI EN 933-1: 1999 to determine the aggregate granulometric curve. The fraction below 63 μm, comprising the binder and the finer aggregate fraction, was mineralogically characterized with X-ray powder diffraction analysis, with associated ethylene glycol treatment for an optimal characterization of the clay fraction of the materials [8]. Finally, the samples were studied by scanning electron microscopy (SEM) for microtextural and microchemical characterization. Semi-quantitative concentration of major elements was determined both on selected areas of the binder and on secondary calcite lumps (when present) using an energy-dispersive X-ray system (EDS). Data allowed the determination of the hydraulicity of the mortar, as measured by the hydraulicity index (HI) [9].

2.2 Results

Based on the petrographic and granulometric analysis the mortars were classified into three groups:

Group 1 (Samples CB, CR, VI; Fig. 1a); these mortars are discernible macroscopically by strong earthy appearance and low coherence. Microscopically, they are composed an inhomogeneous matrix, consisting of cryptocrystalline calcite permeated by an abundant fraction of clay minerals. The aggregate: binder ratio is always about 1:2, and the porosity generally constitutes 20% of the total volume. The filler shows a wide grain-size distribution, ranging from fine gravel to silt, with a bimodal distribution centred on the fine gravel and the fine sand fraction, respectively; the granulometric data determined microscopically are consistent with the results of the granulometric separation (Fig. 2). Both fractions have a predominant carbonate composition, characterised by subrounded to rounded fragments of partially dolomitized spathic and bioclastic limestones. A subordinate siliceous fraction is also present, mainly composed of subangular fragments of quartz and rare clinopyroxene, plagioclase, and K-feldspar crystals.

Group 2 (Samples SE, BA; Fig. 1b); these mortars are discernible macroscopically by a less earthy appearance and a greater coherence with respect to the mortars of Group 1. Microscopically, they are composed of a homogeneous matrix consisting of cryptocrystalline calcite with a low fraction of clay minerals. Submillimetric lumps of secondary calcite, probably due to incomplete mixture of lime with water and aggregate, were also identified. The aggregate: binder ratio is always about 2:1, and the porosity generally constitutes 10% of the total volume. The filler shows a wide grain-size distribution, ranging from fine gravel to silt, with a unimodal distribution centred on the coarse sand fraction; the granulometric data determined microscopically are consistent with the results of the granulometric separation (Fig. 2). This fraction has a predominant siliceous composition, characterised by subrounded to subangular fragments of quartz and

chert with rare clinopyroxene, plagioclase, and K-feldspar crystals and a subordinated carbonate fraction.

Group 3 (sample TE; Fig. 1c); texturally similar to Group 2 mortars, it is discernible by the presence of a local accumulation of clay minerals and the nature of the inert fraction, which is mainly composed of micritic and bioclastic limestone with a very low amount of siliceous fraction.

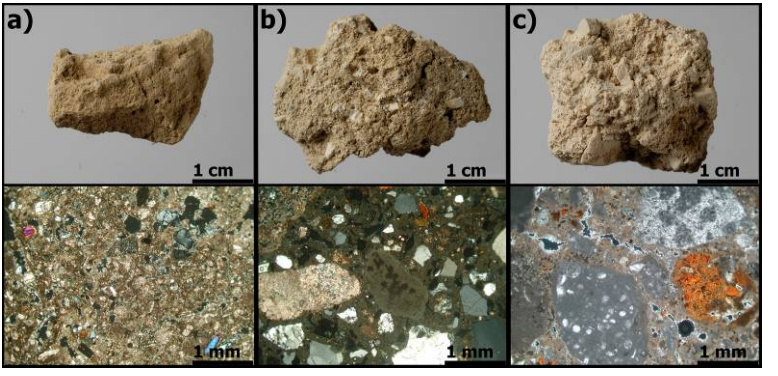

Fig. 1 Macroscopic images and polarising light micrographs (taken in cross polarized light) of the three petrogroups: a) VI sample; b) SE sample; c) TE sample

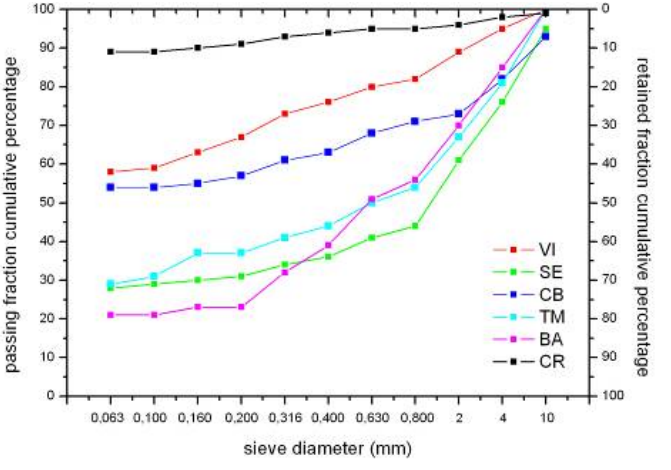

Fig. 2 Original mortars: cumulative size distribution graphs of the aggregate fraction greater than 63 μm

The XRPD analysis of the fine fraction of the mortars gave a mineralogical assemblage with a predominant carbonate fraction, mainly composed of the calcite of the binder, and a subordinate siliceous fraction containing predominant quartz and subordinate feldspar and clinopyroxene. A variable fraction of clay minerals is also present, mainly constituted by illite and subordinate chlorite. The ethylene

glycol treatment showed a consistent fraction of expansive, probably interstratified clays of the smectite group. Semi-quantitative XRPD data, obtained by means of the RIR method, are consistent with the results obtained from the petrographic study: group 1 mortars are characterized by a great amount of clay minerals in the binder fraction, as shown by the scatterplot of the calcite quantity *vs.* the amount of clay minerals (Fig. 3a), while other mortars are distinguishable for the greater purity of the binder matrix. A principal component analysis of the data also was performed (Fig. 3b). The results confirmed the subdivision into the three groups identified by means of petrographic analysis, according to differences in clay content and the mineralogical nature of the finer aggregates.

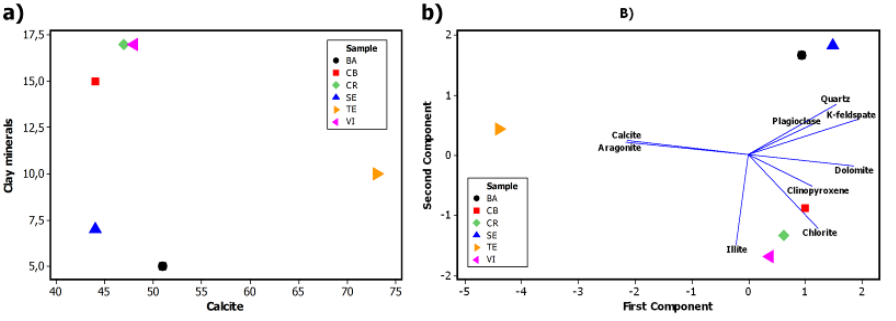

Fig. 3 XRPD semiquantitative data: a) scatter plot of the abundances (mass fraction %) of calcite vs clay minerals; b) Principal component analysis of all the crystalline phases: first two components are plotted (79% of the variance expressed)

Table 1 reports the concentrations of major elements Al, Fe, Si, Ca, and Mg obtained by microchemical analysis of different areas of the binder and that of secondary calcite lumps using SEM-EDS, in addition to the calculated HI. The low values of HI (below 0.1) determined in the majority of mortars, indicate the use of a lime-based air binder for the manufacture of the materials.

Table 1 Mean concentrations of major elements Al, Fe, Si, Ca, and Mg expressed in wt% of the oxide for the binder of the samples analyzed (standard deviation reported in brackets). The suffix –l indicates the analysis was performed on the secondary calcite lumps

Sample	Al_2O_3	Fe_2O_3	SiO_2	CaO	MgO	HI
CB	2.5 (0.80)	1.13 (0.36)	1.59 (0.91)	91.87 (2.82)	2.91 (1.16)	0.05 (0.02)
CR	3.26 (1.22)	1.16 (0.26)	2.73 (1.94)	89.58 (3.1)	3.27 (0.76)	0.07 (0.05)
CR-l	3.99 (1.20)	1.86 (0.01)	6.80 (0.62)	85.21 (2.45)	2.15 (0.80)	0.13 (0.04)
VI	3.36 (0.52)	1.03 (0.04)	3.67 (0.82)	89.09 (1.29)	2.86 (0.21)	0.09 (0.01)
BA	3.35 (1.38)	1.50 (0.17)	2.78 (2.46)	89.68 (4.20)	2.69 (0.66)	0.08 (0.04)
BA-l	3.82 (0.49)	1.34 (0.51)	2.35 (0.28)	89.79 (1.50)	2.71 (0.42)	0.08 (0.01)
SE	3.21 (1.34)	0.66 (0.37)	2.14 (1.38)	91.4 (3.82)	2.93 (1.46)	0.06 (0.02)
SE-l	2.92 (0.34)	1.45 (0.49)	2.26 (0.60)	90.47 (1.07)	2.89 (0.49)	0.07 (0.01)
TE	2.21 (1.00)	0.71 (0.29)	1.35 (0.67)	92.62 (2.25)	2.81 (1.07)	0.04 (0.02)
TE-l	3.09 (0.35)	1.14 (0.10)	3.14 (1.43)	90.39 (0.11)	2.24 (0.87)	0.08 (0.01)

3 Characterization of the restoration grouts

3.1 Materials and methods

For each grout, several test prisms were prepared according to standard UNI EN 196-1: 2005. Half of the prisms were cured *in situ*, while the remaining were cured in laboratory. After an appropriate curing period, the mineralogical assemblage of both *in situ*- and *ex situ*-cured grouts was determined through XRPD to identify possible alteration dynamics. For comparison, XRPD analysis was performed also on anhydrous grouts, coupled with bulk chemical analysis by means of X-ray fluorescence (XRF). Finally, six samples of grouts cured *in situ* were studied by SEM for microtextural and microchemical characterization.

3.2 Results

The grouts were subdivided into three groups according to differences in chemical and mineralogical characteristics:

Group A (MI, M21, AI): grouts based on lime + pozzolanic agent + carbonate microfiller. The anhydrous grouts (Fig. 5a) have a mineralogical assemblage constituted by portlandite and carbonate filler (MI-M21: calcite, AI: dolomite). Two broad bands are also present in the XRD patterns of the grouts: a stronger one peaking at about 31° 2θ and a weaker one peaking at about 48° 2θ. This pattern is typical for the blast furnace slags [10]. The nature of the hydraulic agent is confirmed by the SEM-EDS microanalysis performed on unreacted grains of

slag, consistent with literature data [11]. Considering the intensity of the diffractometric contribution of the slag, the bulk chemical composition of the grouts by XRF (Table 2), the loss on ignition (LOI) data (Table 2), and the visual estimates on quantities of the residual slag grains by SEM-EDS observations (Fig. 4a), it is possible to estimate the use of a comparable quantity of slag for the manufacturing of MI and AI and a greater amount for M21.

The XRD patterns of the hydrated grouts (Fig. 5a) are characterized by the absence of portlandite reflections, associated with the increase of the intensities of the calcite reflections. Moreover, it is possible to observe an increase of the background band at low angle, associated with a series of broad peaks between 8.5° and 12.0° 2θ, which are related to the formation of CSH and AFm cementitious phases, respectively [12]; these data confirm reaction between lime and pozzolanic agent, associated with partial air reaction of portlandite.

No significant differences have been found in the mineralogical assemblage of *in situ*- and *ex situ*-cured grouts, indicating a substantial inertia to chemical degradation phenomena of the materials in the short term. On the other hand, heterogeneity between exposed surfaces and internal portions of the prisms was observed, the latter being characterized by a greenish color. According to literature [13], this phenomenon is related to the release of S^{2-} within the amorphous structure of the slag during the reaction process with portlandite and its subsequent entrance into the crystalline structure of the AFm phases, resulting in the chromophore effect. The chromophore effect disappears on the external portion due to changes in the sulfur oxidation state.

Group B (BC): grout based on hydraulic lime + pozzolanic agent + predominantly siliceous filler. The anhydrous grout (Fig. 5b) has a mineralogical assemblage constituted by C2S (belite) and gehlenite, associated with the aggregate phases (predominantly quartz, subordinately plagioclase, K-feldspar, white mica, serpentine, cordierite, calcite, and dolomite). C2S and gehlenite are the main mineralogical constituents of hydraulic limes produced through calcination of marls at temperatures under 1250° C [12]. SEM-EDS analyses of the aggregate fraction confirmed the predominant siliceous and metamorphic nature of the filler with a subordinate carbonate fraction; the granulometric distribution is unimodal centered on the medium sands granulometric class. Furthermore, SEM observations highlighted the presence of incoherent volcanic scoria fragments (Fig. 4b) mainly constituted by a siliceous-aluminous glass whose chemical composition, determined by EDS, is compatible with the chemical profile of Campi Flegrei pozzolan [14]. This evidence confirms the addition in the mixture of a natural pozzolan as hydraulic agent.

The XRD pattern of the hydrated grout (Fig. 5b) is characterized by the absence of C2S reflections, associated with an increase in the diffractometric contribution of portlandite, CSH, and AFm phases. This evidence confirms both the hydraulic reaction of the low-temperature cementitious phases and the latency of the pozzolanic effect between portlandite and pozzolan in the short term.

A low amount of ettringite and gypsum was found in the grout sample cured *in situ*, indicating a reduced sulfate attack due to reaction between atmospheric sulfates and portlandite and hydrous aluminates in the binder matrix [15].

Group C (O2, O3): ternary grouts based on hydraulic lime + ordinary Portland cement (OPC) + carbonate microfiller. Regarding the binder fraction, the anhydrous grouts have a mineralogical assemblage composed of not only C2S and gehlenite, but also C3S (alite), C3A (aluminate), and C4AF (ferrite) (Fig. 5c), which are the principal mineralogical constituents of the OPC clinker [12]. The presence of cement in the grouts is confirmed by SEM imaging of residual clinker grains (Fig. 4c). An amount of gypsum is also present in the mixture, added to the Portland cement to prevent flash set [12]. Given the intensity of the diffractometric contributions of the clinker phases, the bulk chemical composition of the grouts (in particular Fe_2O_3 and Al_2O_3 content, Table 2), and the visual estimations of quantities of the residual clinker grains by SEM-EDS observations, it is possible to estimate a greater quantity of cement in O2 with respect to O3. The aggregate fraction is composed primarily of carbonates (mostly calcite) and subordinate silicates (mostly quartz). SEM-EDS analyses have evidenced a unimodal granulometric distribution, centered on the silts granulometric class.

The XRD patterns of the hydrated grouts (Fig. 5c) are characterized by the absence of C3S and gypsum reflections and by a reduction in the relative intensities of C2S, C3A, and C4AF reflections, associated with an increasing contribution of CSH and AFm phases, portlandite and ettringite. This evidence confirms the hydraulic reaction of the cementitious phases [12]. Moreover, the greater quantity of portlandite and ettringite in the O2 sample with respect to the O3 sample confirms the higher cement content in the former grout.

No significant differences in the mineralogical assemblage between *in situ* and *ex situ* cured grouts have been found, indicating a substantial inertia to chemical degradation phenomena of the materials in the short term.

Table 2 Bulk chemical composition (obtained by XRF analysis) and LOI of the analyzed grouts

Sample	SiO_2	TiO_2	Al_2O_3	Fe_2O_3	MnO	MgO	CaO	Na_2O	K_2O	P_2O_5	SO_3	LOI
MI	19.78	0.36	7.26	0.46	0.28	4.38	65.45	0.50	0.34	0.07	1.02	23.58
M21	30.74	0.50	11.21	0.45	0.51	6.54	47.65	0.40	0.56	0.01	1.43	4.83
AI	16.79	0.61	8.65	0.48	0.06	22.83	49.25	0.08	0.30	0.02	0.93	34.19
BC	43.30	0.35	7.54	2.54	0.04	2.73	40.57	1.27	1.26	0.06	0.34	19.96
O2	24.77	0.29	5.33	3.45	0.11	2.04	60.21	0.52	1.17	0.10	2.01	13.92
O3	24.50	0.25	4.85	1.63	0.06	1.46	63.25	0.73	0.93	0.08	2.26	18.97

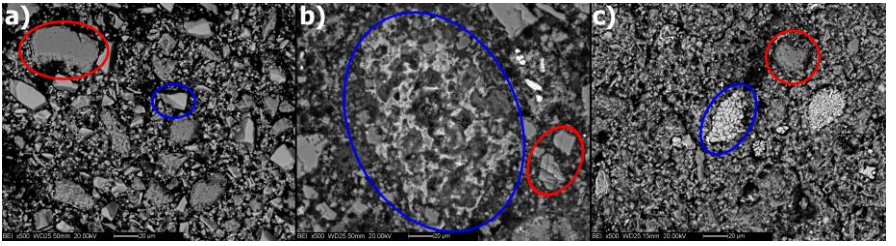

Fig. 4 SEM-BSE images representative for the three groups of grouts: a) group A (MI), unreacted blastfurnace slag fragment circled in blue, carbonate filler circled in red; b) group B (BC), pozzolan fragment circled in blue, siliceous filler circled in red; group C (O3), unhydrated clinker grain circled in blue, carbonate filler circled in red

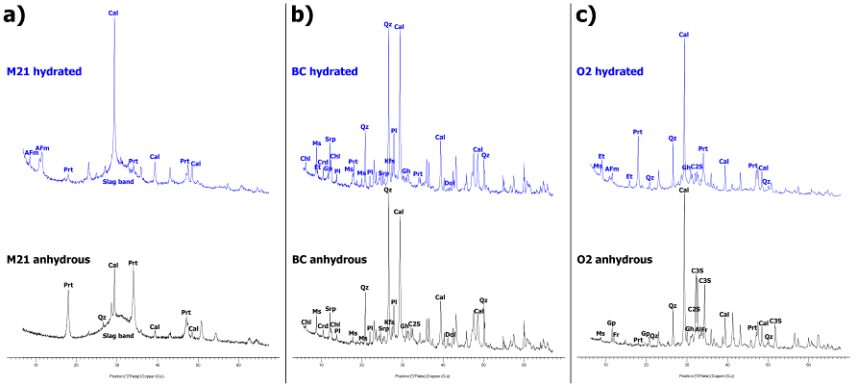

Fig. 5 XRPD patterns representative for the three groups of grouts (anhydrous grouts in black, hydrated grouts in blue). The main reflections of the recognized mineral phases are labelled as: Cal = calcite, Prt = portlandite, Qz = quartz, AFm = AFm cementitious phases, Chl = chlorite, Ms = white mica, Crd = cordierite, Pl = plagioclase, Srp = serpentine, Kfs = K-feldspar, Gh = gehlenite, Dol = dolomite, C2S = belite, Et = ettringite, C3S = alite, Al = aluminate, Fr = ferrite

4 Conclusions

The multianalytical approach led to a good characterization of both the mortars of the investigated historic structures and the selected restoration grouts.

As regards the original mortars, they are all constituted by air lime with an inert fraction compatible, from a minero-petrographic point of view, with the continental deposits of the Aterno river [16]. Moreover, they are discernible in three groups according to binder:aggregate ratio, quantity of dispersed clay fraction in the binder matrix, and compositional and granulometric characteristics of the inert fraction. In particular, the high quantity of clay minerals in group 1 mortars, associated with an enrichment in fine aggregate with respect to the mortars of the other groups, suggests a voluntary addition of soil fraction during

the manufacturing of these materials to reduce production costs, with pernicious effects on the quality of the mortars.

The restoration grouts have been divided into three groups according to minero-petrographic characteristics: group A includes grouts made with lime, blastfurnace slag, and carbonate filler; group B is constituted by a hydraulic lime-based grout with natural pozzolan as hydraulic agent and predominant siliceous filler; group C is composed of ternary grouts with predominantly carbonate filler.

Group A grouts can be considered the most compatible with the original mortars, although the evaluation of their long term resistance is necessary, given the presence in the system of reactive sulfur derived from the slag. Group B grouts can be considered particularly compatible with group 2 mortars, for similarities in the aggregate typology; however, it is necessary to take into account a possible susceptibility of this product to sulfate attack, which has been observed even in the short term. Finally, it is necessary to evaluate the long-term resistance of group 3 grouts, due to possible susceptibilities to chemical attack and incompatibilities with the original mortars related to the presence of cement in the mixtures.

5 References

1. Binda L, Modena C, Baronio G, Abbaneo S (1997) Repair and investigation techniques for stone masonry walls. Constr Build Mater 11(3):133–142
2. Laefer D, Baronio G, Anzani A, Binda L (1998) Measurement of grout injection efficacy for stone masonry walls. Conv. 7 NAMC, Notre Dame, USA, vol 1, pp 484–496Q
3. Vintzileou E, Tassios TP (1995) 'Three leaf stone masonry strengthened by injecting cement grouts.' *J. Structural Eng.*, ASCE, May 1995, 848-856
4. Valluzzi MR, da Porto F, Modena C (2004). "Behavior and modeling of strengthened three-leaf stone masonry walls", RILEM Materials and Structures, MS 267, Vol. 37, April 2004, pp. 184-192.
5. Vintzileou E, Miltiadou-Fezans A (2008) Mechanical properties of three-leaf stone masonry grouted with ternary or hydraulic lime based grouts. Eng Struct 30(8):2265– 2276
6. Kalagri A, Miltiadou-Fezans A, Vintzileou E (2010) Design and evaluation of hydraulic lime grouts for the strengthening of stone masonry historic structures. Mater struct. doi: 10.1617/s11527-009-9572-1
7. Bakolas A, Biscontin G, Contardi V et al (1995) Thermoanalytical research on traditional mortars in Venice. Thermochim Acta 269/270:817-828
8. Martin T (1955) Ethylene Glycol retention by clays. Soil Sci Soc Am J 19:160-164
9. Boynton RS (1966) Chemistry and technology of lime and limestone. Second edition. John Wiley & Sons, New York
10. Regourd M (1986) Characterization and activation of addition product. In: Proceedings of 8th ICCC, Rio de. Janeiro, 1986
11. Demoulian E, Gourdin P, Hawthorn F, Vernet C (1980) Influence of slags chemical composition and texture on their hydraulicity. In: Proceedings of 7th ICCC, Paris, 1980
12. Taylor HFW (2003) Cement Chemistry – 2nd edition. Telford, London
13. Vernet C (1982) Behavior of S^{2-} ions during hydration of slag-rich cements. Silicates Indust. 41:85.
14. Massazza F (1976) Chemistry of pozzolanic additions and mixed cements. Il Cemento 73:3-38

15. Skalny J, Marchand J, Odler I (2003) Sulfate attack on concrete. Spon Press, London
16. Centamore E, Crescenti U, Dramis F (2006) Note illustrative della Carta Geologica d'Italia alla scala 1:50000 - L'Aquila. S.EL.CA., Firenze